Title

A Novel Peptide Prevents Enterotoxin- and Inflammation-Induced Intestinal Fluid Secretion by Stimulating Sodium-Hydrogen Exchanger 3 Activity.

Journal

Gastroenterology, 165(4)

Authors

Zachos, Nicholas

Vaughan, Hannah

Sarker, Rafiquel

et al.

Publication Date

2023-10-01

DOI

10.1053/j.gastro.2023.06.028

Peer reviewed

HHS Public Access

Author manuscript

Gastroenterology. Author manuscript; available in PMC 2024 July 28.

Published in final edited form as:

Gastroenterology. 2023 October ; 165(4): 986–998.e11. doi:10.1053/j.gastro.2023.06.028.

A Novel Peptide Prevents Enterotoxin- and Inflammation-Induced Intestinal Fluid Secretion by Stimulating Sodium-Hydrogen Exchanger 3 Activity

Nicholas C. Zachos[1], **Hannah Vaughan**[2,*], **Ruxian Lin**[1], **Rafiquel Sarker**[1], **Savannah Est-Witte**[2], **Molee Chakraborty**[1,§], **Nicholas W. Baetz**[1], **Hongzhe Yu**[2], **Vladimir Yarov-Yarovoy**[3,4], **George McNamara**[1], **Jordan J. Green**[2], **Chung-Ming Tse**[1], **Mark Donowitz**[1,5]

[1]Division of Gastroenterology and Hepatology, Department of Medicine, Johns Hopkins University School of Medicine, Baltimore, Maryland;

[2]Translational Tissue Engineering Center, Department of Biomedical Engineering, Johns Hopkins University School of Medicine, Baltimore, Maryland;

[3]Department of Physiology and Membrane Biology, University of California Davis, Davis, California;

Correspondence: Address correspondence to: Mark Donowitz, MD, Johns Hopkins University School of Medicine, 720 Rutland Avenue, 925 Ross Research Building, Baltimore, Maryland 21205. mdonowit@jhmi.edu; or Nicholas C. Zachos, PhD, Vanderbilt University Medical Center, 1161 21st Avenue South, D-2306 Medical Center North, Nashville, Tennessee 37232. n.zachos@vumc.org.

*Hannah Vaughan's current affiliation is Medimmune, Gaithersburg, Maryland;

§Molee Chakraborty's current affiliation is St Louis University, St Louis, Missouri.

Supplementary Material

Note: To access the supplementary material accompanying this article, visit the online version of *Gastroenterology* at www.gastrojournal.org, and at https://doi.org/10.1053/j.gastro.2023.06.028.

CRediT Authorship Contributions

Nicholas C. Zachos, PhD (Conceptualization: Equal; Data curation: Supporting; Formal analysis: Supporting; Funding acquisition: Supporting; Investigation: Supporting; Methodology: Supporting; Project administration: Equal; Resources: Supporting; Supervision: Equal; Validation: Supporting; Visualization: Supporting; Writing – original draft: Equal; Writing – review & editing: Equal).

Hannah Vaughan, PhD (Conceptualization: Supporting; Data curation: Supporting; Formal analysis: Supporting; Investigation: Supporting; Methodology: Supporting; Validation: Supporting; Writing – review & editing: Supporting).

Ruxian Lin, MS (Methodology: Supporting; Validation: Supporting; Formal analysis: Supporting; Investigation: Supporting; Data curation: Supporting; Writing – review & editing: Supporting; Visualization: Supporting).

Rafiquel Sarker, PhD (Data curation: Supporting; Formal analysis: Supporting; Investigation: Supporting; Methodology: Supporting; Validation: Supporting).

Savannah Est-Witte, BS (Data curation: Supporting; Investigation: Supporting; Writing – review & editing: Supporting).

Molee Chakraborty, BS (Data curation: Supporting; Formal analysis: Supporting; Investigation: Supporting; Methodology: Supporting; Validation: Supporting).

Nicholas W. Baetz, PhD (Data curation: Supporting; Formal analysis: Supporting; Investigation: Supporting; Methodology: Supporting; Validation: Supporting).

Hongzhe Yu, BS (Data curation: Supporting; Investigation: Supporting).

Vladimir Yarov-Yarovoy, PhD (Data curation: Supporting; Formal analysis: Supporting; Investigation: Supporting; Methodology: Supporting; Visualization: Supporting; Writing – review & editing: Supporting).

George McNamara, PhD (Formal analysis: Supporting; Methodology: Supporting).

Jordan J. Green, PhD (Conceptualization: Supporting; Formal analysis: Supporting; Funding acquisition: Supporting; Project administration: Supporting; Resources: Supporting; Supervision: Supporting; Writing – review & editing: Supporting).

Chung-Ming Tse, PhD (Data curation: Supporting; Formal analysis: Supporting; Investigation: Supporting; Methodology: Supporting; Resources: Supporting; Validation: Supporting).

Mark Donowitz, MD (Conceptualization: Equal; Formal analysis: Supporting; Funding acquisition: Supporting; Investigation: Supporting; Project administration: Equal; Resources: Lead; Supervision: Equal; Writing – original draft: Equal; Writing – review & editing: Equal).

Conflicts of interest

The authors disclose no conflicts.

[4]Department of Anesthesiology and Pain Medicine, University of California Davis, Davis, California;

[5]Department of Physiology, Johns Hopkins University School of Medicine, Baltimore, Maryland

Abstract

BACKGROUND & AIMS: Acute diarrheal diseases are the second most common cause of infant mortality in developing countries. This is contributed to by lack of effective drug therapy that shortens the duration or lessens the volume of diarrhea. The epithelial brush border sodium (Na+)/hydrogen (H^+) exchanger 3 (NHE3) accounts for a major component of intestinal Na^+ absorption and is inhibited in most diarrheas. Because increased intestinal Na^+ absorption can rehydrate patients with diarrhea, NHE3 has been suggested as a potential druggable target for drug therapy for diarrhea.

METHODS: A peptide (sodium-hydrogen exchanger 3 stimulatory peptide [N3SP]) was synthesized to mimic the part of the NHE3 C-terminus that forms a multiprotein complex that inhibits NHE3 activity. The effect of N3SP on NHE3 activity was evaluated in NHE3-transfected fibroblasts null for other plasma membrane NHEs, a human colon cancer cell line that models intestinal absorptive enterocytes (Caco-2/BBe), human enteroids, and mouse intestine in vitro and in vivo. N3SP was delivered into cells via a hydrophobic fluorescent maleimide or nanoparticles.

RESULTS: N3SP uptake stimulated NHE3 activity at nmol/L concentrations under basal conditions and partially reversed the reduced NHE3 activity caused by elevated adenosine 3′,5′-cyclic monophosphate, guanosine 3′,5′-cyclic monophosphate, and Ca^{2+} in cell lines and in in vitro mouse intestine. N3SP also stimulated intestinal fluid absorption in the mouse small intestine in vivo and prevented cholera toxin–, *Escherichia coli* heat-stable enterotoxin–, and cluster of differentiation 3 inflammation–induced fluid secretion in a live mouse intestinal loop model.

CONCLUSIONS: These findings suggest pharmacologic stimulation of NHE3 activity as an efficacious approach for the treatment of moderate/severe diarrheal diseases.

Graphical Abstract

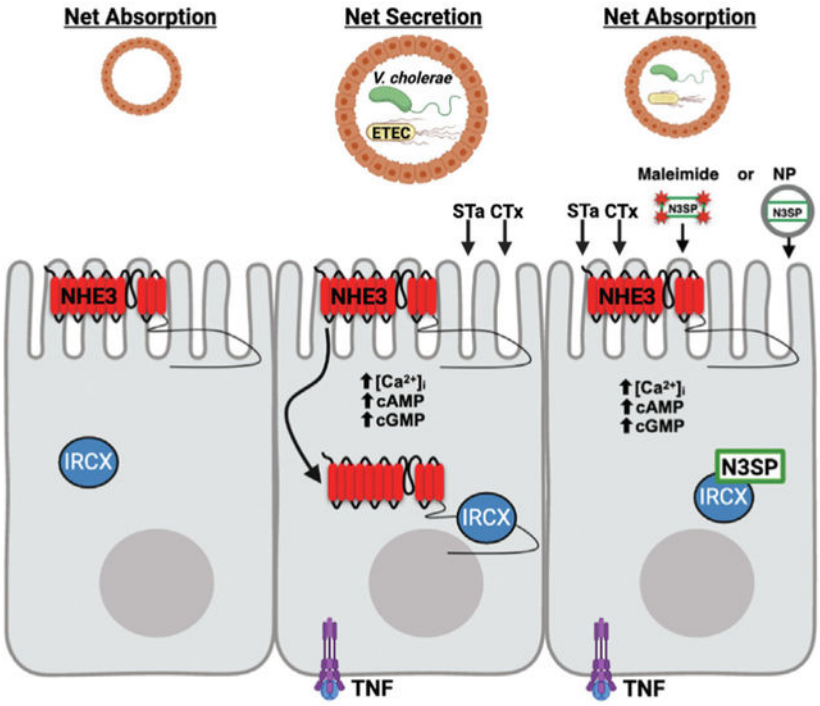

Keywords

NHE3; Intestinal Absorption; Secretion; Enteroids; Diarrhea

The epithelial brush border (BB) sodium (Na^+)/hydrogen (H^+) exchanger 3 (NHE3) accounts for a major fraction of intestinal and renal Na^+ absorption by taking part in the process called neutral NaCl absorption.[1–3] In this process, NHE3 is linked to BB Cl^-/HCO_3^- exchangers of the solute carrier family 26 member (*SLC26A*) gene family, thought to be primarily *SLC26A3*.[4–7] NHE3 is highly regulated as part of digestion, initially being inhibited, which contributes to the spreading of digestive enzymes over the absorptive/digestive surface, and then stimulated later in digestion, which helps avoid postprandial dehydration.[1,3,8–11]

In almost all diarrheal diseases, NHE3 activity is inhibited, mimicking the early stages of digestion, although with a prolonged time course.[10,11] The cyclical inhibition/stimulation of NHE3 occurs via 2 large signaling complexes that form on its intracellular regulatory domain (~aa 455–832).[8,9,12–16] One complex is involved in acute stimulation and the other primarily in acute inhibition. Previous studies conducted by us and others have defined a region of the NHE3 C-terminus (aa 586–605) that interacts primarily with proteins that inhibit NHE3 activity; although some NHE3 stimulatory proteins bind in this area as well.[9,14–18] The significance of this site has been confirmed by mutational studies and interactions validated by coprecipitation experiments and in vitro binding studies with NHE3 C-terminus truncated to aa 605, but not aa 585. Proteins that interact with NHE3 at this site include calcium/calmodulin-dependent protein kinase type II-δ, casein kinase 2, Na^+/H^+ exchanger regulatory factors 1 to 4, phosphoinositide phospholipase C-γ, and

calmodulin (Figure 1A),[13,16] whereas inositol 1,4,5 triphosphate (IP3) receptor binding protein released with IP3 (IRBIT) binds to NHE3 between aa 585 and aa 689. Based on these studies, we hypothesized and tested that a NHE3 mimetic peptide based on this largely inhibitory region might be a putative competitor of protein-protein interactions of the inhibitory regulatory complex, which would result in pharmacologic stimulation of NHE3 activity. An ideal mimetic peptide should (1) be cell permeant, (2) work at low concentrations, (3) increase basal NHE3 activity, with or without inhibiting adenosine 3′,5′-cyclic monophosphate (cAMP), guanosine 3′,5′-cyclic monophosphate (cGMP), calcium- and inflammation-mediated inhibition of NHE3 activity, and (4) alter Na^+/H^+ activity in a specific manner. If successful, this mimetic could be a candidate drug for treating diarrheal diseases.

Materials and Methods

NHE3 inhibitory domain (Figure 1A) mimicking peptides were synthesized by Peptide 2.0 (Chantilly, VA), and purity was assessed to be >98% by high-performance liquid chromatography. Peptides include (see Figure 1B) (1) control peptide (CP) 1, (2) NHE3 stimulatory peptide 1 (N3SP-1), (3) N3SP-1Δ7, and (4) CP-2 (N3SP-1Δ10). A C-terminal cysteine was added to the peptides for conjugation to 4,4-difluoro-1,3,5,7,8-pentamethyl-4-bora-3a,4a-diaza-*s*-indacene (BODIPY) 577/618. For nanoparticle uptake studies, an N-terminal biotin was added to CP-2 and N3SP-1Δ7. Additional methods are in the Supplementary Methods.

Results

Computational Modeling and Engineering of Sodium-Hydrogen Exchanger 3 Mimetic Peptides

We previously defined that aa 586–605 (rabbit NHE3) of the intracellular C-terminal domain is the region that directly binds proteins that inhibit NHE3 activity. We termed this the NHE3 inhibitory regulatory complex (IRCX) (Figure 1A).[12,13,15] We hypothesized that a peptide mimic of this region would competitively bind proteins of the NHE3 IRCX, reduce their association with NHE3, and prevent NHE3 inhibition. To test this, we synthesized a 21 aa peptide representing aa 585 to 605 of rabbit NHE3 (CP-1) (Figure 1B) with an additional C-terminal Cys to conjugate BODIPY 577/618, a fluorescent maleimide that when conjugated to a peptide/protein, renders the peptide cell-permeable and fluorescent at the wave lengths studied (Supplementary Figure 1A).[18,19] CP-1 was exposed to PS120/HA_3-NHE3/sodium-hydrogen exchange regulatory cofactor 2 (NHERF2) cells, and peptide entry was confirmed by confocal microscopy (Figure 2A).[18,19] However, there was no significant effect of CP-1 (400 nmol/L) compared with BODIPY alone on basal NHE3 activity (Figure 2B).

A bioinformatics approach was used to provide insight into aa immediately upstream or downstream from the CP-1 boundaries, considering that adjacent aa might allow increased competition with the IRCX for binding regulatory proteins. Models of the 3-dimensional structure of the sequence of the NHE3 C-terminus around the domain involved in binding members of the NHE3 IRCX were created using the Rosetta structural modeling software

(see Methods[20–22]). Extending the N-terminal sequence of CP-1 to aa 568, while keeping the C-terminal aa 605, predicted a stable structure composed of 2 alpha helixes with H^+ bonding between R^{575} and D^{602} that stabilized the helices (Supplementary Figure 2A). This peptide was named N3SP-1. Removing up to 7 amino acids from the N-terminus of this peptide preserved the ability to stimulate NHE3 activity (Table 1). Removal of ≥8 aa was predicted to lose the hydrogen bonding and result in peptide instability (shown for N3SP-1Δ10 in Supplementary Figure 2A) and loss of NHE3 stimulatory activity (Table 1). Multiple sequence alignments of NHE3 from multiple species were generated, demonstrating preservation of aa in this area of NHE3 (Supplementary Figure 2B).

Functional Characterization of Sodium-Hydrogen Exchanger 3 Mimetic Sodium-Hydrogen Exchanger 3 Stimulatory Peptide 1 Compared With Control Peptide 1

In vitro studies—BODIPY conjugates.—BODIPY-conjugated N3SP-1 (Figure 2A–E) was assayed for effects on NHE3 activity when loaded into PS120/HA_3-NHE3/NHERF2 cells (Figure 2B), Caco-2/BBe/HA_3-NHE3 cells (Figure 2C), and in vitro mouse jejunum (Figure 2D). Intracellular loading was documented by confocal microscopy (Figure 2A). CP-1 was used as the negative control in these studies. In all models, N3SP-1 (400 nmol/L) stimulated basal NHE3 activity compared with CP-1 (Figure 2B–D). No stimulatory effect was detected with exposure to unconjugated N3SP-1 (Supplementary Figure 1B). The range of stimulation was 41% to 61% (PS120, 61% [Figure 2B]; Caco-2/BBe, 41% [Figure 2C]; and mouse jejunum, 57% [Figure 2D]). Increased basal NHE3 activity in Caco-2/BBe/HA_3-NHE3 cells was concentration dependent, with maximal effect at 400 nmol/L and a 50% effective concentration (EC_{50}) of 152 nmol/L (Figure 2E).

Further studies examined the effect of N3SP-1 on acute NHE3 inhibition by Ca^{2+} ionophore 4-Br-A23187, forskolin (FSK), and carbachol, as well as acute stimulation by epidermal growth factor. N3SP-1 pretreatment prevented inhibition of NHE3 by 0.5 μmol/L A23187 in PS120 fibroblasts (Figure 2B), FSK (10 μmol/L) in Caco-2/BBe cells and mouse jejunum in vitro (Figure 2C and D), and carbachol (10 μmol/L) in Caco-2/BBe cells (Figure 2C), but did not alter epidermal growth factor (200 ng/mL) stimulation in Caco-2/BBe cells (38% vs 35% stimulation in presence of CP-1 vs N3SP-1, respectively) (Figure 2C). The loss of FSK inhibition on NHE3 activity in Caco-2/BBe cells had a similar concentration-dependent response to that on basal NHE3 activity, with EC_{50} of 157 nmol/L after addition apically to Caco-2/BBe cells (Figure 2E). These results demonstrate that N3SP-1, but not CP-1, prevents cAMP- and Ca^{2+}-mediated inhibition of NHE3 activity in vitro. We next determined whether N3SP-1 exerts similar effects in vivo.

In vivo studies—BODIPY conjugates.—The effect of the N3SP-1 was determined in live mouse models, measuring net water transport under basal conditions and in 2 bacterial enterotoxin-induced (ie, cholera toxin[CTx] and *Escherichia coli* heat-stable enterotoxin) diarrheal disease closed-loop models (Figure 3). Acute exposure of mouse jejunum to N3SP-1 (400 nmol/L) via intraluminal perfusion[23] acutely stimulated basal water absorption compared with CP-1. In a typical experiment, jejunal net water transport was 4.2 $\mu L \cdot min^{-1} \cdot cm^{-1}$ with CP-1 and 50.3 $\mu L \cdot min^{-1} \cdot cm^{-1}$ with N3SP-1; the difference in net water

transport between N3SP-1 and CP-1 perfused jejunal loops was 56.6 ± 15.1 $\mu L \cdot min^{-1} \cdot cm^{-1}$ (n 5; $P = .0004$).

In the closed-loop model, purified CTx (1 μg/3- to 4-cm loop) was instilled in the presence of 400 nmol/L N3SP-1 or CP-1 for 6 hours, and then net fluid secretion (loop weight/cm) was determined (Figure 3A). N3SP-1 prevented CTx-stimulated fluid secretion, whereas CP-1 did not alter fluid accumulation compared with CTx alone (Figure 3A). This effect of N3SP-1 on CTx-induced secretion was associated with visible intracellular accumulation of the peptide after 6 hours of exposure and contrasted to the localization of CP-1, which remained at the BB (Figure 3B). This difference in peptide localization was associated with differential localization of NHE3. Confocal microscopy (Figure 3B) showed NHE3 was internalized in the CTx-treated mouse jejunum when exposed to CP-1. In contrast, NHE3 was detected on the CTx-treated jejunal BB after exposure to N3SP-1. These results suggest that reduced luminal fluid accumulation in CTx-treated mouse intestinal loops by N3SP-1 is associated with increased BB expression of NHE3 compared with CP-1.

The N3SP-1 effect so dramatically reduced the CTx-induced fluid secretion that specificity of the effect was determined, despite the fact that N3SP-1 is part of the NHE3 C-terminus and is not matched by any other protein sequence, as assessed by BLAST. This was done by measuring the short-circuit current (Isc) in loops exposed to CTx for 6 hours in the presence of phosphate-buffered saline (PBS), CP-1, or N3SP-1 added at the same time as CTx (Supplementary Figure 3A). Changes in Isc were then determined in treated loops after sequential exposure to basolateral FSK, followed by carbachol, with peak Isc determined after exposure of each agonist. The assumption was that if N3SP-1 inhibited cystic fibrosis transmembrane conductance regulator (CFTR) activity, Isc would be significantly lower in loops exposed to CTx plus N3SP-1 compared with loops exposed to CTx in PBS or CP-1, as well as possibly demonstrating less subsequent stimulation of Isc by FSK or carbachol. In fact, the Isc in CTx-treated loops exposed to CP-1 and N3SP-1 was slightly, but not significantly, greater than in the loops treated with CTx in PBS, and there was no significant difference in Isc of the CTx plus CP-1 or NS3P-1 loops (Supplementary Figure 3A). In addition, the peak increases in Isc in CTx-exposed loops with sequential addition of FSK and carbachol were not different between the CP-1– and N3SP-1–exposed loops (Supplementary Figure 3B). These results support that N3SP-1 does not inhibit CTx-induced Cl^- secretion mediated by cAMP or Ca^{2+} signaling but rather that N3SP-1 effects involve stimulation of Na^+ absorption. We next determined whether this beneficial effect occurs in other murine diarrheal disease models.

E coli heat-stable enterotoxin-induced mouse jejunal fluid accumulation, a cGMP-dependent effect,[24,25] was studied. *E coli* purified heat-stable enterotoxin (0.5 μg) caused intestinal fluid accumulation that was significantly reduced by N3SP-1 (Figure 3C). This effect was not observed when heat-stable enterotoxin–treated loops were exposed to CP-1. Thus, N3SP-1 not only stimulates basal NHE3 activity and net jejunal water absorption but also prevents changes in net water secretion caused by 2 major bacterial enterotoxins responsible for cholera and Traveler's Diarrhea.

We next determined whether N3SP-1 exhibits similar effects in a previously standardized diarrheal model of tumor necrosis factor-α–mediated inflammation (via anti-cluster of differentiation [CD] 3 monoclonal antibodies).[23] Mouse jejunal loops were prepared containing 100 μL PBS with 400 nmol/L CP-1 or N3SP-1. After surgery, 200 μL PBS alone or with 200 μg anti-CD3 antibody were injected intraperitoneally, and mice were euthanized 2.5 hours later. Anti-CD3 antibody increased luminal fluid accumulation in loops containing CP-1 but not in NS3P-1 loops (Figure 3D). This demonstrates that N3SP-1 also prevents fluid secretion in an inflammatory diarrhea model. This effect was not specific for sex (Supplementary Figure 3C).

Because in silico modeling of N3SP-1 suggested a potential interaction between rabbit R^{575} and D^{602}, we determined whether R^{575} was necessary for N3SP-1 effects. Purified peptides were synthesized that lack the first 7 (N3SP-1Δ7) or 10 (CP-2) N-terminal amino acids of N3SP-1, where only N3SP-1Δ7 contains R^{575} (Figure 1B and Supplementary Figure 2A). These peptides were tested in CTx loops, except that 400 nmol/L CP-2 and N3SP-1Δ7 were used (Figure 3E). Results similar to those with N3SP-1 and CP-1 were found, supporting that deletion of the N-terminal 7 amino acids of N3SP-1 did not alter the efficacy of this peptide to reduce CTx-related diarrhea.

Nanoparticle Delivery of Sodium-Hydrogen Exchanger 3 Stimulatory Peptide-1 Into Ex Vivo Human Jejunal Enteroid Monolayers

Because maleimide conjugation does not represent a viable delivery system for human use, nanoparticle delivery of CP-2 and N3SP-1Δ7 was tested in human jejunal enteroid monolayers. Polymeric nanoparticles comprised hyperbranched carboxylated poly(β-amino) ester (PBAE) with carboxylate ligand end caps were selected[26–28] (Supplementary Figure 4A). This class of polymers enables efficient cellular uptake, endosomal escape, and cytosolic delivery of various proteins ranging from 27 to 160 kDa in size.[27] Hyperbranched PBAE polymer is advantageous as a biomaterial for intracellular delivery due to its pH responsiveness, low cytotoxicity, and biodegradability.[28] Further, the polymer used for this study, termed CR5 (Supplementary Figure 4A), incorporates bioreducible disulfide bonds in the polymer backbone, which facilitates efficient triggered release of cargo preferentially in the cytosol, where glutathione concentrations are significantly elevated relative to the extracellular environment.[29] Nanoparticle synthesis, characterization, and pH effects on toxicity and cellular uptake in the B16-F10 cancer cell line are described in Supplementary Figure 4A–I.

Given the effectiveness of N3SP-1Δ7 in preventing CTx-induced net fluid secretion in mouse intestine in vivo, enteroid studies were performed to demonstrate nanoparticle uptake into human intestinal epithelial cells. Optimized nanoparticle formulations containing CP-2 or N3SP-1Δ7 were added apically to differentiated human jejunal enteroid monolayers. Fluorescently labeled nanoparticle location was identified by confocal microscopy and compared with endogenous apical NHE3. Nanoparticles appeared intracellularly, confirming uptake in normal human intestinal epithelial cells (Figure 4A). Similar studies were performed in B16-F10 cells, demonstrating time- and concentration-dependent uptake,

whereas in the absence of nanoparticles, no significant uptake occurred (Supplementary Figure 4G).

For functional studies, we considered that in vitro delivery of nucleotides by PBAE nanoparticles peaked within 24 to 48 hours of nanoparticle exposure.[27] Thus, nanoparticles were added apically (250 nmol/L) for 18 hours to differentiated enteroid monolayers, and the effect on basal and FSK-inhibited NHE3 activity was determined. NHE3 activity was significantly increased in N3SP-1Δ7 compared with CP-2 (increase of 36.0% ± 10.4%, n = 4; $P = .043$). FSK significantly reduced NHE3 activity in CP-2–exposed enteroids (77.2% ± 7.4% of control peptide, n = 4; $P = .048$) (Figure 4B). In contrast, in N3SP-1Δ7–exposed enteroids, FSK caused a nonsignificant decrease in NHE3 activity (88.0% ± 6.7% of N3SP-1, n = 4; $P = .170$).

To further interrogate the loss of the FSK effect, whether the FSK stimulation of adenylate cyclase-cAMP was altered by N3SP-1Δ7 was determined. In jejunal enteroids exposed to FSK, increased intracellular cAMP was similar between CP-2 and N3SP-1Δ7 (Figure 4C). This demonstrates that the prevention of FSK inhibition of NHE3 occurred downstream of FSK-stimulated adenylate cyclase-increased cAMP. Thus, as observed with maleimide-based delivery of N3SP-1, nanoparticle delivery in human enteroids stimulated basal NHE3 activity and prevented cAMP inhibition of NHE3.

Given the ability of N3SP-1Δ7 to prevent CTx-induced fluid secretion in vivo (Figure 3E) and to stimulate basal NHE3 activity and prevent cAMP inhibition in human enteroids (Figure 4C), further studies were done with human enteroids to determine the shortest N3SP-1–related peptide that would stimulate human NHE3. A series of N3SP-1 N-terminal truncations was synthesized, and concentration-dependent stimulation of NHE3 activity was determined using human jejunal enteroids. As summarized in Table 1, deleting 5, 6, or 7 aa from the N3SP-1 N-terminus produced peptides that stimulated NHE3 similarly to full-length N3SP-1 both in magnitude of the stimulation and EC_{50}. However, removing 8 aa significantly reduced the maximum stimulatory effect and increased the EC_{50}, whereas removing more than 8 aa totally prevented NHE3 stimulation.

In Vivo Studies—Nanoparticle Conjugates and Intestinal Fluid Absorption

To treat acute diarrhea, the drug effect should have a rapid onset. Consequently, the effects of the nanoparticle-conjugated CP-2 compared with N3SP-1Δ7 was determined on net fluid transport in closed 3- to 4-cm ileal loops exposed to 400 nmol/L peptide for 4 hours, followed by draining of the loops and exposure to 150 μL PBS for 30 minutes. As shown in Figure 5A, N3SP-1Δ7 incubation produced significantly less residual fluid, consistent with increased fluid absorption. To demonstrate that this was due to increased Na^+ absorption that involved NHE3 caused by N3SP-1Δ7, these closed-loop studies were repeated with the specific NHE3 inhibitor[30,31] tenapanor (10 μmol/L), present during both incubation periods. In the presence of tenapanor, there was no difference in residual fluid comparing CP-2 and N3SP-1Δ7 (compare Figure 5A and B).

An additional study was performed to determine whether nanoparticle-N3SP pretreatment could prevent CTx-induced fluid secretion. Nanoparticle–N3SP-1Δ7 or CP-2 (4 μmol/L)

with 0.1 μg CTx in 150 μL PBS were inoculated into closed mouse ileal loops, as above. The animals were euthanized 4 hours later, and loop weight/length determined. Loops only injected with CTx and PBS or PBS alone with the same total volume as the nanoparticle-injected loops were studied as additional controls. As shown in Figure 5C, NS3P-1Δ7 loops had significantly less fluid at 4 hours than the other 2 conditions. CP-2 did not reduce the residual loop volume. Subtracting the PBS-only loop weight/length from the CTx-incubated loops indicated the NS3P-1Δ7 reduced the CTx-induced secretion by ~42%. This effect was associated with preventing CTx-induced NHE3 trafficking from the BB (Supplementary Figure 5), suggesting a similar mechanism of action occurs with nanoparticle-delivered N3SP and BODIPY-conjugated N3SP (compare with Figure 3B). This demonstrates that as with the BODIPY–N3SP-1 studies, nanoparticle–N3SP-1Δ7 reduced CTx-induced intestinal fluid secretion.

Sodium-Hydrogen Exchanger 3 Peptide–Sodium-Hydrogen Exchange Regulatory Cofactor 2 Overlay Experiments: Effects of Control Peptide 2 and Sodium-Hydrogen Exchanger 3 Stimulatory Peptide-1Δ7 Peptides

To further test the hypothesis that N3SP-1 stimulated NHE3 by competing for binding with components of the IRCX, overlay experiments were performed examining binding of NHERF2 to NHE3 peptides. NHERF2 is a 2 PDZ (postsynaptic density 95, Discs large; Zonula occludens 1) domain-containing scaffold that is involved in intestinal NHE3 stimulation and inhibition and is part of the IRCX.[12–15,31] Binding of purified full-length glutathione-*S*-transferase–NHERF2 to 2 maltose-binding protein–NHE3 C-terminal peptides that contain the N3SP-1 sequence was determined in the presence of equal concentrations of CP-2 compared with N3SP-1Δ7. CP-2 and N3SP-1Δ7 peptides were used at 5 times the concentration of the NHERF2 fusion protein and the maltose-binding protein–NHE3 fusion peptides. N3SP-1Δ7 significantly reduced NHERF2 binding compared with the control peptide (Figure 6).

Discussion

This study strongly supports NHE3 as a druggable target for treatment of diarrheal diseases in which NHE3 is inhibited, but present. NHE3 is inhibited in almost all diarrheal diseases, including secretory and inflammatory diarrheal diseases.[3,14,15] In fact, whereas stimulated anion secretion is considered to be the major contributor to volume loss in secretory diarrheal diseases, such as cholera and Traveler's Diarrhea, this does not appear to be the case for inflammatory diarrheal diseases, including inflammatory bowel diseases or radiation enteritis, among others.[10,11] Here we describe a peptide that stimulates basal NHE3 activity and prevents NHE3 inhibition caused by elevated cAMP, cGMP, and Ca^{2+}, second messengers known to inhibit NHE3 and to be intermediates in human diarrheal diseases. Multiple intestinal models were studied that included in vivo and in vitro mouse intestine as well as in cell lines, including fibroblasts expressing NHE3, the polarized human colon cancer cell line Caco-2/BBe, and ex vivo normal human jejunal enteroids.[9,14,24,25,31,32] We used these cell, tissue, animals, and human enteroids to model secretory and inflammatory diarrheal diseases, including 2 models of bacterial enterotoxin-induced secretion and a model of tumor necrosis factor-α–related secretion. All models

produced similar evidence of the effectiveness of NS3P to stimulate basal NHE3 activity and to reverse the inhibition that occurs in each of the diarrhea models studied, while at the same time reducing the overall fluid secretion. In addition, we determined that the efficacy of N3SP in stimulating NHE3 activity, which does not enter epithelial cells alone, required conjugation to a cell-penetrating maleimide or to nanoparticles, because there was no effect without cell entry. Moreover, we showed that N3SP-stimulated basal and second messenger inhibited NHE3 similarly at very low concentrations (EC_{50} ~150 nmol/L) using either delivery system.

Some insights have been provided from these studies concerning the mechanism(s) by which N3SP stimulates basal NHE3 activity and reverses NHE3 inhibition in the in vivo models of intestinal fluid secretion. Under normal conditions, NHE3 continually traffics between the endosomal system and the plasma membrane, with the percentage on the BB determined by the balance between rates of endocytosis, exocytosis, and BB protein stability.[1–3,8,14,15] The diarrhea-related inhibition of NHE3 is usually due to abnormal trafficking caused by agents that induce the diarrhea, which act by elevating intracellular cAMP, cGMP, Ca^{2+}, all of which stimulate rates of NHE3 endocytosis and often also inhibit exocytosis.[1–3,12,13,33–36]

N3SP was engineered to mimic the intracellular NHE3 C-terminal domain that binds proteins to form the largest identified NHE3 regulatory complex, which is primarily involved in inhibiting NHE3 activity. This sequence of NHE3 is unique in the human genome, and thus, we predicted that it would allow effects specific for NHE3. Our studies show that N3SP interferes in the reduction of apical NHE3 expression caused by the diarrheal disease models studied as the consequence of its mechanism of action.

The proposed mechanism of N3SP stimulation of NHE3 is to compete with proteins that normally bind to the NHE3 C-terminus in the inhibitory domain and prevent their binding under basal conditions and with elevated second messenger signaling. Proteins shown to bind to this area of NHE3 and inhibit basal NHE3 activity include the kinase calmodulin-dependent protein kinase II-δ, calmodulin, phospholipase C-γ, and NHERFs 1 to 4.[12–14,17,18] IRBIT-1, which also regulates NHE3 activity,[37] binds just the C-terminal of this area. That this is the mechanism involved in N3SP effects on NHE3 is supported by the reduced binding caused by N3SP compared with the control peptide of one of the major components of the NHE3 IRCX, NHERF2, to peptides of the NHE3 C-terminus that contain the N3SP sequence (Figure 6). More detailed studies are required to identify all components of the IRCX and the effects of N3SP on their interactions with the NHE3 C-terminus, although that is beyond the scope of this study. The lack of structural information of the 2 NHE3 C-terminus fusion proteins prevents any insights on why effects of NS3P compared with control peptide were greater in competing with NHERF2 peptide in the larger NHE3 peptide.

Not understood is the important ability of N3SP-1 to completely prevent the fluid secretion induced in vivo by CTx, *E coli* heat-stable enterotoxin, and anti-CD3–induced inflammation. Enterotoxin-induced Cl^- secretion, which is dependent on activation of CFTR, is thought to be the major component of cholera and enterotoxigenic *E coli* secretory diarrheas.[3,10,11] We were unable to identify any evidence that N3SP did other than stimulate NHE3, with the

in vivo stimulation of NHE3 confirmed by the effect on basal transport being prevented by tenapanor pretreatment (Figure 5). N3SP-1 did not inhibit the FSK stimulation of adenylate cyclase-cAMP in enteroids and did not alter the Isc in CTx-exposed mouse jejunum or the subsequent stimulation induced sequentially by FSK and carbachol, making an effect to inhibit stimulated Cl^- secretion unlikely.

Unlike CFTR, NHE3 has not been shown to be directly involved in regulation of other transport proteins. The only regulatory functions of NHE3 identified relate to its generation of an apical membrane H^+ gradient, which provides some of the driving force of peptide transporter 1 uptake of di-, tri-, and oligopeptides and some H^+ gradient-linked amino acid transporters,[38,39] and separately, stimulation of intestinal phosphate absorption, apparently by effects on specific tight junctional permeability to phosphate.[40] Nonetheless, this is an area requiring further exploration testing the hypothesis that NHE3 is indirectly involved in the regulation of other transport processes that contribute to fluid secretion in diarrheal diseases. Another possible explanation for these findings is that whereas the stimulated Cl^- secretory process has been believed to be greater in magnitude than Na^+ absorptive processes, perhaps in vivo, the opposite is true.

Structural information about the NHE3 C-terminus would allow us to understand why N3SP-1/N3SP-1Δ7 but not CP-1/CP-2 stimulates NHE3 activity. Despite advances by cryogenic electron microscopy in understanding the structure of mammalian as well as bacterial NHEs, there is very little experimental structural information concerning the NHE3 C-terminus distal to the proximal domain that binds calcineurin homologous protein that is adjacent to the transmembrane domain.[41–45]

In addition, the recently reported remarkable ability of the AlphaFold Protein Structural Database (European Molecular Biology Laboratory–European Bioinformatics Institute) to define protein structure from amino acid sequences has been used to describe the structure of NHE3.[46] This method predicted a structure of the NHE3 C-terminal domain similar to our Rosetta model, although this was in an area that the program described as “low confidence.”[46] The Rosetta structural model allowed us to engineer a peptide that stimulated NHE3 with a low EC_{50} (~150 nmol/L). This model predicated that the stability of N3SP-1 was based on the peptide forming two alpha helixes, which were stabilized by H^+ bonding between human R^{576} and E^{602} (in rabbit R^{575} and D^{602}).

Although structural stability has not been experimentally confirmed, truncation of N3SP-1 to form N3SP-1-NΔ7 (N terminal amino acid R^{575}) preserved NHE3 stimulation with a similar EC_{50} to N3SP-1 in enteroids, whereas efficacy was greatly reduced by removing one more N-terminal aa. This model predicts continued stability of the N3SP-1-NΔ7 by the same H^+ bonding as N3SP-1, and that R^{575} at the beginning of the first helix in aa 575–605 is important for preserving functional ability of N3SP to stimulate NHE3 activity. This model also predicts decreased stability by removing R^{575}, as occurs with the N3SP-1Δ8 peptide. Of note, the N-terminal region in CP-1 (residues 585–605) appears to form a flexible structure, supporting the assumption that a stable helical structure is important for the N3SP stimulation of NHE3 activity.

Considering the findings presented in this study together, we suggest that N3SP should be considered for further development as an antidiarrheal drug. An important observation was similar EC_{50} for NHE3 stimulation by N3SP-1 in a human colon cancer line and normal human enteroids, which we have suggested as a potential way to assess potential human drug efficacy.[47–49]

Nanoparticles were used as a delivery vehicle for potential human use of N3SP. Nanoparticle delivery into the human colon cancer cell line, Caco-2 and rat small intestine has been demonstrated, and PBAE nanoparticles have been shown to deliver nucleic acids into human embryonic kidney and B16-F10 cancer cells.[27,28] The peak delivery by PBAE nanoparticles of nucleic acids occurred 24 to 48 hours after nanoparticle exposure.[27] Mimicking this application, our initial studies with nanoparticle delivery of N3SP-1Δ7 was after overnight exposure.

Until now, we have not pursued oral delivery of N3SP-1Δ7 or considered in detail issues of acid stability to pass through the stomach (Supplementary Figure 4H indicates pH stability in preliminary studies), or release at specific segments of the small intestine or colon, which are the sites responsible for most diarrheal diseases. However, these considerations have been dealt with for peptide therapies, such as linaclotide and plenalotide, and for numerous other drugs, such as budesonide; and consequently, we consider these are the next stage of development of N3SP-1Δ7 as a drug. In addition, further potential uses of N3SP-1Δ7 include as a tool to identify the components of the signaling complexes that regulate NHE3 and for further mechanistic studies to define the role of N3SP as an antidiarrheal drug. Importantly, the efficacy of NS3P should be tested in additional diarrhea models to define the range of potentially treatable diarrheas.

Supplementary Material

Refer to Web version on PubMed Central for supplementary material.

Acknowledgments

Mark Donowitz and Nicholas C. Zachos should be considered as co-corresponding authors. We acknowledge the role of Drs Damian van Rossum and Randen L. Patterson (Pennsylvania State University) who used a bioinformatics program they developed called Adaptive-Blast to model the areas of the NHE3 C-terminus to suggest areas to consider for peptide boundaries, and Yoojin Hong (Pennsylvania State University) for initial computational analyses of the NHE3-terminal structure.

Funding

This work was supported by NIH/NIBIB P41 EB028239 (JJG), NIH/NIDDK RO1 DK26523 (MD), RO1 DK116352 (MD), R24 DK099803 (MD), Digestive Disease Research Core Center Grant P30 DK089502 (MD), Bill and Melinda Gates Foundation (MD, NCZ), TEDCO Maryland Innovation Commercialization Program (NCZ), and a grant with the Pennsylvania Department of Health using Tobacco Settlement Funds (DVR).

Data Availability

All data are available in the original manuscript and online Supplementary Material.

Abbreviations used in this paper:

BB	brush border
BODIPY	4,4-difluoro-1,3,5,7,8-pentamethyl-4-bora-3a,4a-diaza-*s*-indacene
cAMP	adenosine 3′,5′-cyclic monophosphate
CD	cluster of differentiation
CFTR	cystic fibrosis transmembrane conductance regulator
cGMP	guanosine 3′,5′-cyclic monophosphate
cPBAE	carboxylated branched poly(beta-amino) ester
CP-1	control peptide 1
CTx	cholera toxin
EC_{50}	50% effective concentration
FSK	forskolin
IRBIT	inositol 1,4,5 triphosphate (IP3) receptor binding protein released with IP3
IRCX	inhibitory regulatory complex
Isc	short-circuit current
N3SP-1	sodium-hydrogen exchanger 3 stimulatory peptide 1
NHE3	sodium-hydrogen exchanger 3
NHERF-2	sodium-hydrogen exchange regulatory cofactor 2
PBAE	poly(β-amino) ester
PBS	phosphate-buffered saline

References

1. Zachos NC, Kovbasnjuk O, Foulke-Abel J, et al. Human enteroids/colonoids and intestinal organoids functionally recapitulate normal intestinal physiology and pathophysiology. J Biol Chem 2016;291:3759–3766. [PubMed: 26677228]
2. Rao MC. Physiology of electrolyte transport in the gut: implications for disease. Compr Physiol 2019;9:947–1023. [PubMed: 31187895]
3. Zachos NC, Tse M, Donowitz M. Molecular physiology of intestinal Na+/H+ exchange. Annu Rev Physiol 2005; 67:411–443. [PubMed: 15709964]
4. Walker NM, Simpson JE, Yen PF, et al. Down-regulated in adenoma Cl/HCO3 exchanger couples with Na/H exchanger 3 for NaCl absorption in murine small intestine. Gastroenterology 2008;135:1645–1653.e3. [PubMed: 18930060]
5. Xia W, Yu Q, Riederer B, et al. Human enteroids/colonoids and intestinal organoids functionally recapitulate normal intestinal physiology and pathophysiology. Pflugers Arch 2014;466:1541–1556. [PubMed: 24233434]

6. Musch MW, Arvans DL, Wu GD, et al. Functional coupling of the downregulated in adenoma Cl-/base exchanger DRA and the apical Na+/H+ exchangers NHE2 and NHE3. Am J Physiol Gastrointest Liver Physiol 2009;296:G202–G210. [PubMed: 19056765]
7. Haggie PM, Cil O, Lee S, et al. SLC26A3 inhibitor identified in small molecule screen blocks colonic fluid absorption and reduces constipation. JCI Insight 2018;3: e121370. [PubMed: 30046015]
8. Kapus A, Grinstein S, Wasan S, et al. Functional characterization of three isoforms of the Na+/H+ exchanger stably expressed in Chinese hamster ovary cells. ATP dependence, osmotic sensitivity, and role in cell proliferation. J Biol Chem 1994;269:23544–23552. [PubMed: 8089122]
9. Levine SA, Montrose MH, Tse CM, et al. Kinetics and regulation of three cloned mammalian Na+/H+ exchangers stably expressed in a fibroblast cell line. J Biol Chem 1993;268:25527–25535. [PubMed: 8244988]
10. Camilleri M, Sellin JH, Barrett KE. Pathophysiology, evaluation, and management of chronic watery diarrhea. Gastroenterology 2017;152:515–532.e2. [PubMed: 27773805]
11. Barrett KE. Epithelial transport in digestive diseases: mice, monolayers, and mechanisms. Am J Physiol Cell Physiol 2020;318:C1136–C1143. [PubMed: 32293934]
12. Donowitz M, Li X. Regulatory binding partners and complexes of NHE3. Physiol Rev 2007;87:825–872. [PubMed: 17615390]
13. Donowitz M, Mohan S, Zhu CX, et al. NHE3 regulatory complexes. J Exp Biol 2009;212:1638–1646. [PubMed: 19448074]
14. Sarker R, Grønborg M, Cha B, et al. Casein kinase 2 binds to the C terminus of Na+/H+ exchanger 3 (NHE3) and stimulates NHE3 basal activity by phosphorylating a separate site in NHE3. Mol Biol Cell 2008; 19:3859–3870. [PubMed: 18614797]
15. Akhter S, Kovbasnjuk O, Li X, et al. Na(+)/H(+) exchanger 3 is in large complexes in the center of the apical surface of proximal tubule-derived OK cells. Am J Physiol Cell Physiol 2002;283:C927–C940. [PubMed: 12176749]
16. Hendus-Altenburger R, Kragelund BB, Pedersen SF. Structural dynamics and regulation of the mammalian SLC9A family of Na(+)/H(+) exchangers. Curr Top Membr 2014;73:69–148. [PubMed: 24745981]
17. Zizak M, Chen T, Bartonicek D, et al. Calmodulin kinase II constitutively binds, phosphorylates, and inhibits brush border Na+/H+ exchanger 3 (NHE3) by a NHERF2 protein-dependent process. J Biol Chem 2012; 287:13442–13456. [PubMed: 22371496]
18. Zachos NC, van Rossum DB, Li X, et al. Phospholipase C-gamma binds directly to the Na+/H+ exchanger 3 and is required for calcium regulation of exchange activity. J Biol Chem 2009;284:19437–19444. [PubMed: 19473983]
19. Boehning D, van Rossum DB, Patterson RL, et al. A peptide inhibitor of cytochrome c/inositol 1,4,5-trisphosphate receptor binding blocks intrinsic and extrinsic cell death pathways. Proc Natl Acad Sci U S A 2005;102:1466–1471. [PubMed: 15665074]
20. Bender BJ, Cisneros A 3rd, Duran AM, et al. Protocols for molecular modeling with Rosetta3 and RosettaScripts. Biochemistry 2016;55:4748–4763. [PubMed: 27490953]
21. Rohl CA, Strauss CE, Misura KM, et al. Protein structure prediction using Rosetta. Methods Enzymol 2004; 383:66–93. [PubMed: 15063647]
22. Bonneau R, Strauss CE, Rohl CA, et al. De novo prediction of three-dimensional structures for major protein families. J Mol Biol 2002;322:65–78. [PubMed: 12215415]
23. Clayburgh DR, Musch MW, Leitges M, et al. Coordinated epithelial NHE3 inhibition and barrier dysfunction are required for TNF-mediated diarrhea in vivo. J Clin Invest 2006;116:2682–2694. [PubMed: 17016558]
24. Sunuwar L, Yin J, Kasendra M, et al. Mechanical stimuli affect *Escherichia coli* heat-stable enterotoxin-cyclic GMP signaling in a human enteroid intestine-chip model. Infect Immun 2020;88:e00866–19. [PubMed: 31818966]
25. Foulke-Abel J, Yu H, Sunuwar L, et al. Phosphodiesterase 5 (PDE5) restricts intracellular cGMP accumulation during enterotoxigenic *Escherichia* coli infection. Gut Microbes 2020;12:1752125.
26. Kozielski KL, Tzeng SY, Green JJ. A bioreducible linear poly(beta-amino ester) for siRNA delivery. Chem Commun (Camb) 2013;49:5319–5321. [PubMed: 23646347]

27. Rui Y, Wilson DR, Choi J, et al. Carboxylated branched poly (beta-amino ester) nanoparticles enable robust cytosolic protein delivery and CRISPR-Cas9 gene editing. Sci Adv 2019;5:eaay3255.
28. Wilson DR, Rui Y, Siddiq K, et al. Differentially branched ester amine quadpolymers with amphiphilic and pH-sensitive properties for efficient plasmid DNA delivery. Mol Pharm 2019;16:655–668. [PubMed: 30615464]
29. Karlsson J, Tzeng SY, Hemmati S, et al. Photo-crosslinked bioreducible polymeric nanoparticles for enhanced systemic siRNA delivery as cancer therapy. Adv Funct Mater 2021;31(17):2009768.
30. Spencer AG, Labonte ED, Rosenbaum DP, et al. Intestinal inhibition of the Na+/H+ exchanger 3 prevents cardiorenal damage in rats and inhibits Na+ uptake in humans. Sci Transl Med 2014;6:227ra36.
31. Jacobs JW, Leadbetter MR, Bell N, et al. Discovery of tenapanor: a first-in-class minimally systemic inhibitor of intestinal Na+/H+ exchanger isoform 3. ACS Med Chem Lett 2022;13:1043–1051. [PubMed: 35859876]
32. Murtazina R, Kovbasnjuk O, Chen TE, et al. NHERF2 is necessary for basal activity, second messenger inhibition, and LPA stimulation of NHE3 in mouse distal ileum. Am J Physiol Cell Physiol 2011;301:C126–C136. [PubMed: 21430287]
33. Yin J, Sunuwar L, Kasendra M, et al. Fluid shear stress enhances differentiation of jejunal human enteroids in Intestine-Chip. Am J Physiol Gastrointest Liver Physiol 2021;320:G258–G271. [PubMed: 33074011]
34. Donowitz M, Janecki A, Akhter S, et al. Short-term regulation of NHE3 by EGF and protein kinase C but not protein kinase A involves vesicle trafficking in epithelial cells and fibroblasts. Ann N Y Acad Sci 2000;915:30–42. [PubMed: 11193592]
35. Chow CW, Khurana S, Woodside M, et al. The epithelial Na(+)/H(+) exchanger, NHE3, is internalized through a clathrin-mediated pathway. J Biol Chem 1999; 274:37551–37558. [PubMed: 10608808]
36. Chen T, Kocinsky HS, Cha B, et al. Cyclic GMP kinase II (cGKII) inhibits NHE3 by altering its trafficking and phosphorylating NHE3 at three required sites: identification of a multifunctional phosphorylation site. J Biol Chem 2015;290:1952–1965. [PubMed: 25480791]
37. He P, Zhang H, Yun CC. IRBIT, inositol 1,4,5-triphosphate (IP3) receptor-binding protein released with IP3, binds Na+/H+ exchanger NHE3 and activates NHE3 activity in response to calcium. J Biol Chem 2008; 283:33544–33553. [PubMed: 18829453]
38. Thwaites DT, Anderson CM. H+-coupled nutrient, micronutrient and drug transporters in the mammalian small intestine. Exp Physiol 2007;92:603–619. [PubMed: 17468205]
39. Watanabe C, Kato Y, Ito S, et al. Na+/H+ exchanger 3 affects transport property of H+/oligopeptide transporter 1. Drug Metab Pharmacokinet 2005;20:443–451. [PubMed: 16415530]
40. King AJ, Siegel M, He Y, et al. Inhibition of sodium/hydrogen exchanger 3 in the gastrointestinal tract by tenapanor reduces paracellular phosphate permeability. Sci Transl Med 2018;10:eaam6474.
41. Ben Ammar Y, Takeda S, Sugawara M, et al. Crystallization and preliminary crystallographic analysis of the human calcineurin homologous protein CHP2 bound to the cytoplasmic region of the Na+/H+ exchanger NHE1. Acta Crystallogr Sect F Struct Biol Cryst Commun 2005; 61:956–958.
42. Ammar YB, Takeda S, Hisamitsu T, et al. Crystal structure of CHP2 complexed with NHE1-cytosolic region and an implication for pH regulation. EMBO J 2006; 25:2315–2325. [PubMed: 16710297]
43. Pang T, Su X, Wakabayashi S, et al. Calcineurin homologous protein as an essential cofactor for Na+/H+ exchangers. J Biol Chem 2001;276:17367–17372. [PubMed: 11350981]
44. Sjøgaard-Frich LM, Prestel A, Pedersen ES, et al. Dynamic Na(+)/H(+) exchanger 1 (NHE1) – calmodulin complexes of varying stoichiometry and structure regulate Ca(2+)-dependent NHE1 activation. Elife 2021;10: e60889. [PubMed: 33655882]
45. Winklemann I, Matsuoka R, Meier PF, et al. Structure and elevator mechanism of the mammalian sodium/proton exchanger NHE9. EMBO J 2020;39:e105908. [PubMed: 33118634]

46. Tunyasuvunakool K, Adler J, Wu Z, et al. Highly accurate protein structure prediction for the human proteome. Nature 2021;596:590–596. [PubMed: 34293799]

47. Donowitz M, Turner JR, Verkman AS, et al. Current and potential future applications of human stem cell models in drug development. J Clin Invest 2020;130: 3342–3344. [PubMed: 32452833]

48. Cil O, Phuan PW, Gillespie AM, et al. Benzopyrimidopyrrolo-oxazine-dione CFTR inhibitor (R)-BPO-27 for antisecretory therapy of diarrheas caused by bacterial enterotoxins. FASEB J 2017;31:751–760. [PubMed: 27871064]

49. Duan T, Cil O, Tse CM, et al. Inhibition of CFTR-mediated intestinal chloride secretion as potential therapy for bile acid diarrhea. FASEB J 2019;33:10924–10934. [PubMed: 31268738]

WHAT YOU NEED TO KNOW

BACKGROUND AND CONTEXT

Drug treatments for diarrheal diseases are inadequate. Inhibition of the brush border sodium-hydrogen exchanger 3 contributes to pathophysiology of almost all diarrheal diseases. Sodium-hydrogen exchanger 3 is regulated by multiprotein complexes, one of which inhibits its activity.

NEW FINDINGS

A peptide (sodium-hydrogen exchanger 3 stimulatory peptide 1) duplicating the sodium-hydrogen exchanger 3 domain, which forms the inhibitory complex, was loaded into intestinal cells linked to a maleimide or to nanoparticles and stimulated baseline sodium-hydrogen exchanger 3 activity and reversed sodium-hydrogen exchanger 3 inhibition caused by adenosine 3′,5′-cyclic monophosphate, guanosine 3′,5′-cyclic monophosphate, Ca^{2+}, bacterial enterotoxins, and inflammation.

LIMITATIONS

Mechanistically, it is not known why sodium-hydrogen exchanger 3 stimulatory peptide 1 not only stimulated sodium-hydrogen exchanger 3 baseline and diarrhea-related sodium-hydrogen exchanger 3 inhibited activity but also turned off multiple forms of intestinal fluid secretion.

CLINICAL RESEARCH RELEVANCE

Acute diarrheal diseases are the second most common cause of infant mortality in developing countries. This is contributed to by lack of effective drug therapy that shortens the duration or lessens the volume of diarrhea. Sodium-hydrogen exchanger 3 accounts for a major component of intestinal Na^{+} absorption and is inhibited in most diarrheas. Sodium-hydrogen exchanger 3 stimulatory peptide 1, which alters sodium-hydrogen exchanger 3 activity at nanomolar concentrations, is a potential drug for treating multiple causes of diarrhea.

BASIC RESEARCH RELEVANCE

Sodium-hydrogen exchanger 3 is regulated by large, multiprotein signaling complexes. Sodium-hydrogen exchanger 3 stimulatory peptide 1 stimulation of sodium-hydrogen exchanger 3 activity prevented binding of a major part of the inhibitory complex and its use will allow probing how the signaling complex forms to regulate sodium-hydrogen exchanger 3. The reversal of the fluid secretion in multiple diarrhea models requires understanding of the relative magnitude of the absorptive and secretory processes in intact intestine.

A.

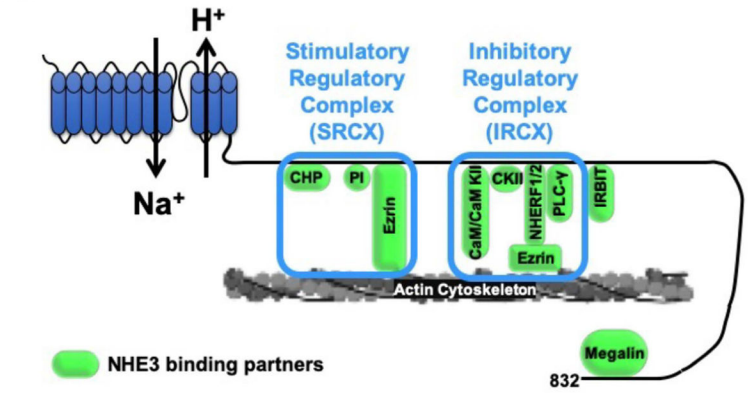

B.

NAME	Amino Acid Composition of Peptides Studied
CP-1	^{585}YLLRESASAVCLDMQSLEQRR^{605}-C
N3SP-1	^{568}NVDFSTPRPSTVEASVSYLLRESASAVCLDMQSLEQRR^{605}-C
N3SP-1Δ7	^{575}RPSTVEASVSYLLRESASAVCLDMQSLEQRR^{605}-C
CP-2 (N3SP-1Δ10)	^{578}TVEASVSYLLRESASAVCLDMQSLEQRR^{605}-C

Figure 1.

N3SP-1 is part of the NHE3 C-terminus, which forms the IRCX. (*A*) Domain structure of NHE3 modified from[13,16] showing N-terminal transport domain and C-terminal regulatory domain, including suggested boundaries for the binding of the IRCX. The boxes indicate proteins shown to directly bind to the NHE3 C-terminus in the area of the stimulatory and inhibitory regulatory complexes. Amino acid refers to rabbit NHE3. (*B*) Peptides mimicking the NHE3 amino acids that make up the IRCX binding domain (AA refers to rabbit NHE3). CaM, calmodulin; CaM KII, calmodulin-dependent protein kinase II; CHP, calcineurin homologous protein; PLC-γ, phospholipase C-γ.

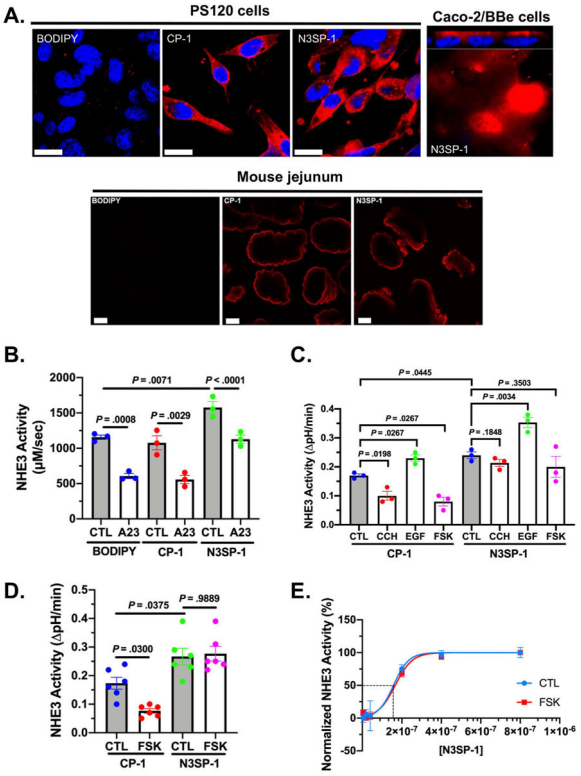

Figure 2.

Effect of N3SP-1 on basal and acutely stimulated and inhibited NHE3 activity. (*A*) Confocal microscopy shows uptake of BODIPY-conjugated N3SP-1 and CP-2 in PS120/HA_3-NHE3/NHERF2 cells (*top, left*), Caco-2/BBe cells (*top, right*), and mouse jejunum (*bottom*; 2-photon microscopy). BODIPY (*top, left*) is not conjugated to either peptide and is not fluorescent.[18,19] Red, BOPIDY-conjugated peptides; blue, nuclei. Scale bars = 20 μm. (*B*) Effect of N3SP-1 compared with CP-1 and with BODIPY alone (all studied at 400 nmol/L) on basal and 4-Br-A23187 inhibition of NHE3 activity in PS120/HA_3-NHE3/NHERF2 cells. Results are rates of NHE3 activity (μmol · L^{-1} · s^{-1}) shown as mean ± standard error of the mean of 3 experiments (paired *t* tests). CTL, control. (*C*) NHE3 activity in polarized Caco-2/BBe/HA_3-NHE3 cells exposed to 400 nmol/L CP-1 or N3SP-1, both studied under basal conditions, after 5-minute exposure to 10 μmol/L carbachol (CCH), 30-minute exposure to 25 μmol/L FSK, or 30-minute exposure to 200 ng/mL epidermal growth factor (EGF) (n = 3 for all experiments; paired *t* tests for comparison with cells treated only with CP-1 or N3SP-1). (*D*) NHE3 measured in mouse jejunum in vitro studied with 2 photon microscope/SNARF-4F under basal conditions and after 30-minute exposure to 25 μmol/L FSK with exposure to 400 nmol/L CP-1 or N3SP-1 (n = 6; unpaired *t* tests). (*E*) Kinetic analysis of N3SP-1 stimulation of basal NHE3 activity (blue; EC_{50} = 152 nmol/L) and prevention of FSK inhibition of NHE3 (red; EC_{50} = 157 nmol/L). EC_{50} calculated by Hill equation.

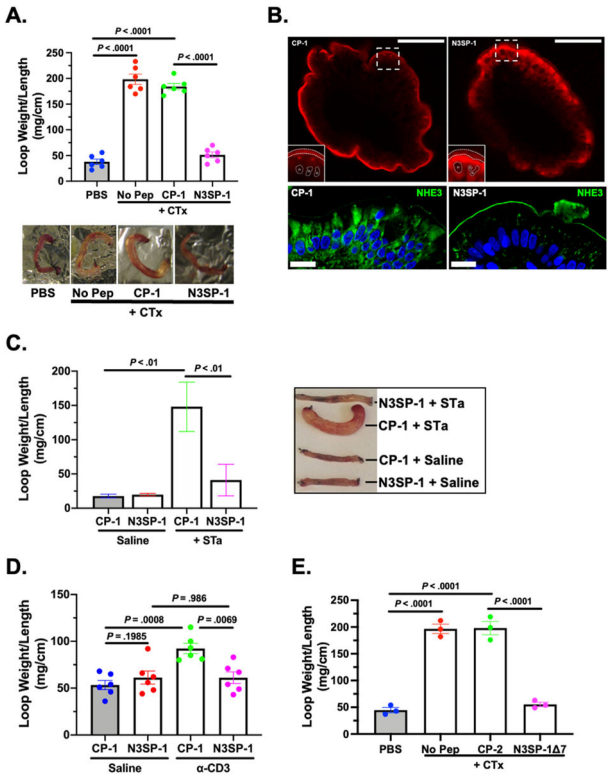

Figure 3.

N3SP-1 prevents net mouse jejunal fluid secretion induced by CTx, *Escherichia coli* heat-stable enterotoxin, and anti-CD3 monoclonal antibody-induced inflammation. (*A*) Fluid accumulation (loop weight/length) 6 hours after inoculation of jejunal loops containing 1 μg purified CTx in presence of 400 nmol/L CP-1, N3SP-1, or PBS. *P* values are comparison with loops inoculated with only PBS by paired *t* tests. Results from at least 2 loops from 6 animals per condition. Representative loop distention shown *below*. (*B*) Intracellular localization of N3SP-1 in mouse jejunum 6 hours after loop inoculation with 1 μg CTx with 400 nmol/L CP-1 or N3SP-1 (*upper*) and localization of NHE3 under the same conditions (*below*). Scale bars = 20 μm. (*C*) Fluid accumulation (loop weight/length) 4 hours after inoculation of 3- to 4-cm jejunal loops with 0.5 μg purified *E coli* heat-stable (STa) enterotoxin in the presence of 400 nmol/L CP-1, N3SP-1, or saline. *P* values are comparison with loops inoculated with only saline by paired *t* tests. Results from at least 2 loops from 6 animals per condition. Representative loop distention is shown. (*D*) Fluid accumulation (loop wet weight/length) 2.5 hours after intraperitoneal injection of 200 μL saline or anti-CD3 antibody in mice with 2 jejunal loops containing 400 nmol/L CP-1 or N3SP-1. *P* values are comparison of loops inoculated with CP-1 compared with N3SP-1 and loops from intraperitoneal saline vs CD3 antibody by paired *t* tests. Results from 6 animals injected with saline and 6 with anti-CD3 antibody (total of 12 loops studied containing CP-1 or N3SP-1). (*E*) Studies performed as in panel *A* with CTx exposure but with 400 nmol/L CP-2 and N3SP-1Δ7 (n = 3). *P* values are comparison with PBS-inoculated loops by paired *t* tests. Data are shown as mean ± standard error of the mean.

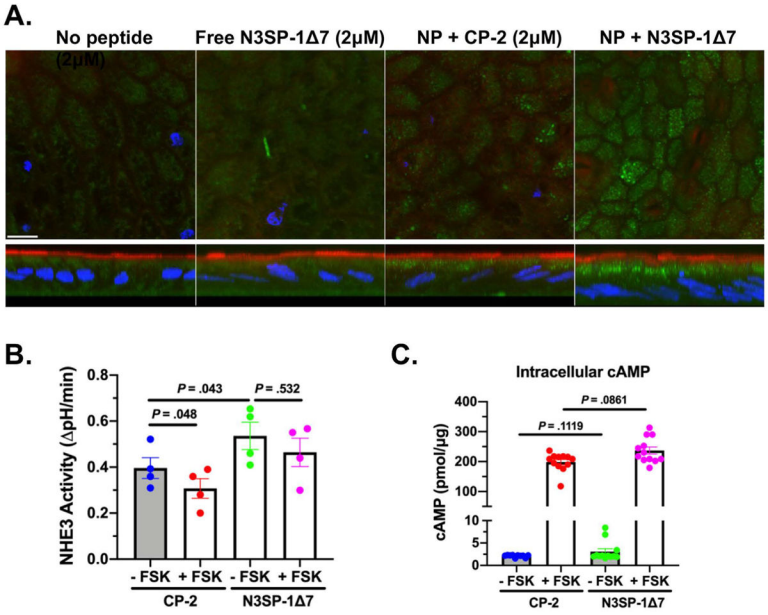

Figure 4.

Nanoparticles–CP-2 and N3SP-1Δ7 are taken up by differentiated human duodenal enteroids, stimulate basal NHE3 activity, and prevent cAMP inhibition of NHE3 activity. (*A*) Confocal microscopy of fluorescently labeled nanoparticles (PBAE CR5 30:1 w/w nanoparticles:peptide) (2 μmol/L, 4-hour uptake after apical addition to differentiated enteroid monolayers) revealed predominantly subapical location of nanoparticles (green) (XY sections *above*; XZ sections *below*). Nanoparticles (NP) were labeled with streptavidin–Alexa Fluor 488-conjugated peptides. Endogenous NHE3 (red; anti–NHE3-Alexa Fluor 567) marked the apical domain. Note lack of uptake of N3SP-1Δ7 in the absence of conjugation to nanoparticles (*left panel*). Scale bar = 10 μm. (*B*) Differentiated enteroid monolayers were exposed to nanoparticle–CP-2 or N3SP-1Δ7 (250 nmol/L) overnight, and NHE3 activity was measured under basal conditions or after FSK exposure (n = 4; paired *t* tests). (*C*) Adenylate cyclase-cAMP levels were measured on enteroid monolayers treated as in panel *B*, comparing results from 12 monolayers from 3 experiments. *P* values from unpaired *t* tests. Data are shown as mean ± standard error of the mean.

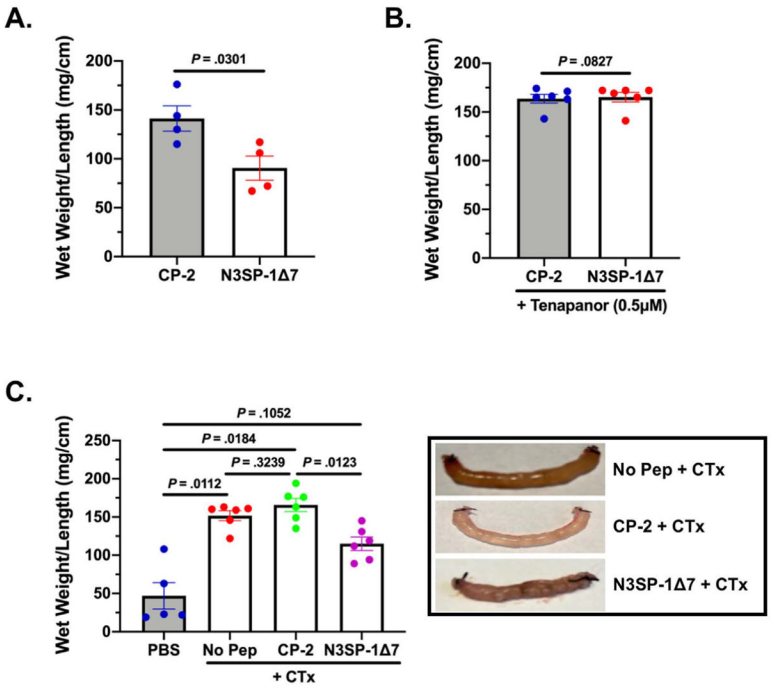

Figure 5.

Nanoparticle-conjugated N3SP-1Δ7 stimulates NHE3 and reduces CTx-induced fluid secretion in vivo. (*A*) Closed-loop absorption studies of fluid absorption over 30 minutes in in vivo mouse proximal small intestine after 4-hour exposure to nanoparticle-peptide (400 nmol/L) demonstrated that N3SP-1Δ7 compared with CP-2 increased fluid absorption. (*B*) The N3SP-1Δ7 increased baseline fluid absorption was prevented by pretreatment with 10 μmol/L tenapanor (n = 4 and 3 separate experiments for *A* and *B*, respectively, with 8 animals studied for *A* and 12 for *B*). (C) At 4 hours after CTx (0.1 μg) exposure, net fluid secretion was determined in ileal loops also inoculated only with PBS, nanoparticles–CP-2 (4 μmol/L) or nanoparticles–N3SP-1Δ7 (4 μmol/L) (n = 6). *P* values compared with PBS/CTx loops by unpaired *t* tests. In parallel, ileal loops only exposed to PBS represent an additional control (n = 5). Data are shown as the mean ± standard error of the mean.

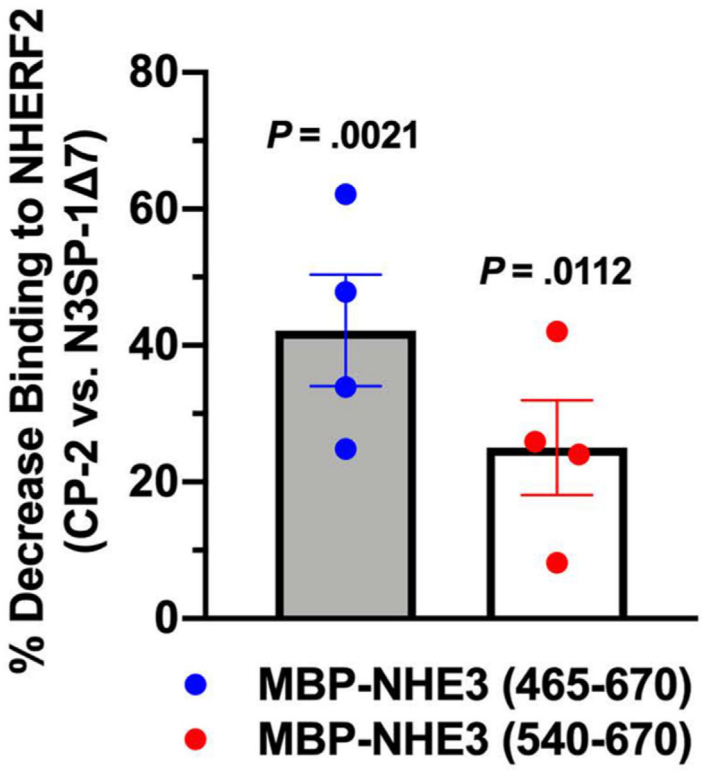

Figure 6.

N3SP-1Δ7 preferentially reduces NHERF2 binding to NHE3 peptides in in vitro overlay assays. Two NHE3 C-terminal peptides containing the N3SP-1 sequence were separated on sodium dodecyl sulfate-polyacrylamide gel electrophoresis gradient gels, and purified NHERF binding was determined. Equal concentrations of NHE3 peptides and NHERF2 were used. Before NHERF2 addition, the blots were overlayed with 5× the concentration of N3SP-1Δ7 vs CP-2. The test peptide competed with NHERF2 binding significantly more than the control peptide (n = 5). *P* values from unpaired *t* tests. Data are shown as the mean ± standard error of the mean.

Table 1.

Effect of N-Terminal Truncations of Sodium-Hydrogen Exchanger 3 Stimulatory Peptide 1 on Sodium-Hydrogen Exchanger 3 Activity in Human Duodenal Enteroids

N3SP-1 variant	Stimulation of NHE3 activity (%)	EC_{50}
N3SP-1	Yes (38)	152 nmol/L
N3SP-1Δ18	No	
CP-2 (N3SP-1Δ10)	No	
N3SP-1Δ9	No	
N3SP-1Δ8	Yes (9)	356 μmol/L
N3SP-1Δ7	Yes (39)	156 nmol/L
N3SP-1Δ6	Yes (40)	151 nmol/L
N3SP-1Δ5	Yes (39)	154 nmol/L

NOTE. Concentration-dependent effects on NHE3 basal activity was determined using BCECF-fluorometry. Kinetic analysis was determined of extent of stimulation of basal NHE3 activity; analysis was by use of Hill equation. Truncation of 5, 6, or 7 N-terminal aa did not significantly alter the magnitude of the stimulation of NHE3 or alter the EC_{50}; however, truncation of 8 aa reduced the stimulatory effect and significantly increased the EC_{50}, whereas further truncations of 9, 10, and 18 aa produced peptides that were without effect on basal NHE3 activity.